International Journal of Information, Control and Computer Sciences
ISSN: 2517-9942
Vol:7, No:8, 2013

Sensorless Backstepping Control Using an Adaptive Luenberger Observer with Three Levels NPC Inverter

A. Bennassar, A. Abbou, M. Akherraz, M. Barara

***Abstract*—**In this paper, we propose a sensorless backstepping control of induction motor (IM) associated with three levels neutral clamped (NPC) inverter. First, the backstepping approach is designed to steer the flux and speed variables to theirs references and to compensate the uncertainties. A Lyapunov theory is used and it demonstrates that the dynamic trajectories tracking are asymptotically stable. Second, we estimate the rotor flux and speed by using the adaptive Luenberger observer (ALO). Simulation results are provided to illustrate the performance of the proposed approach in high and low speeds and load torque disturbance.

***Keywords*—**Sensorless backstepping, IM, Three levels NPC inverter, Lyapunov theory, ALO.

I. Introduction

THE induction motor has been widely used in various industrial applications due to its high reliability, relativity low cost and easy maintenance requirements. However, its nonlinear structure requires decoupled torque and flux control. Several methods of control are used to control the induction motor among which the field orientation control (FOC) that allows a decoupling between the flux and the torque in order to obtain an independent control of the flux and the torque like dc motors [1]. However, the control of dynamical systems in presence of uncertain and disturbances is a common problem when algorithms of classical regulation such as proportional-integral controllers are used to control speed, flux and currents. Recently, several nonlinear control approaches have been introduced. One of these approaches that have been applied to induction motor control is the backstepping design [2], [3].

The backstepping is a systematic and recursive design methodology for nonlinear feedback control. The idea of backstepping design is to select recursively some appropriate functions of state variables as pseudo-control inputs for lower dimension subsystems of the overall system. Each backstepping stage results in a new pseudo-control design, expressed in terms of the pseudo-control designs from preceding design stages. Lyapunov functions associated with each individual design stage to ensure the global stability of the system [4].

The sensorless speed control of induction motor has received over the last few years a great interest. Thus it is necessary to eliminate the speed sensor to reduce hardware and increase mechanical robustness. In traditional approaches, the flux and the speed is estimated using the stator voltage and currents, but this can provide a large error in speed estimation, including very low speeds [5], [6]. The main techniques of sensorless control of induction motors are: model reference adaptive systems (MRAS), extended Kalman filter (EKF) and adaptive flux observer (ALO). In this paper, the ALO is used for the estimation of the rotor flux and speed of an induction motor. This estimator can be used for the joint state and parameter estimation of a nonlinear dynamic system. In the ALO, which is a deterministic observer, the rotor flux and speed to estimate is considered as states [7].

This paper is organized as follow: the induction motor oriented model is described in Section II, Section III reviews the backstepping control design, Section IV highlights the three levels npc inverter, in Section V the estimation of the rotor speed and flux using adaptive Luenberger observer is discussed. Finally, simulations result and conclusion are given in Sections VI, VII.

II. Induction Motor Oriented Model

In field oriented control, the flux vector is forced to align with d-axis ($\Phi_{rq} = \frac{d\Phi_{rq}}{dt} = 0$). Thus, the induction motor model in (d-q) reference frame can be given by the following state equations:

$$\begin{aligned}
\frac{di_{sd}}{dt} &= -\gamma i_{sd} + \omega_s i_{sd} + p\Omega i_{sq} + \frac{\mu}{T_r}\varphi_{rd} + \frac{L_m}{T_r}\frac{i_{sq}^2}{\varphi_{rd}} + \frac{1}{\sigma L_s}v_{sd} \\
\frac{di_{sq}}{dt} &= -\gamma i_{sq} - \omega_s i_{sq} - p\Omega i_{sd} - \mu p\Omega\varphi_{rd} - \frac{L_m}{T_r}\frac{i_{sq}i_{sd}}{\varphi_{rd}} + \frac{1}{\sigma L_s}v_{sq} \\
\frac{d\varphi_{rd}}{dt} &= \frac{L_m}{T_r}i_{sd} - \frac{1}{T_r}\varphi_{rd} \\
\frac{d\Omega}{dt} &= \eta\Phi_{rd}i_{sq} - \frac{f}{J}\Omega - \frac{C_r}{J}
\end{aligned} \tag{1}$$

with:

$$\gamma = \left(\frac{R_s}{\sigma L_s} + \frac{1-\sigma}{\sigma T_r}\right) \; ; \; T_r = \frac{L_r}{R_r} \; ; \; \mu = \frac{L_m}{\sigma L_s L_r} \; ; \; \eta = \frac{pL_m}{JL_r} \; ; \; \sigma = 1 - \frac{L_m^2}{L_s L_r}$$

A. Bennassar is with Mohamed V University, Mohammadia School's of Engineers, Av. Ibn Sina P.B 765 Agdal, Rabat, Morocco (e-mail: ab.bennassar @gmail.com).

A. Abbou, M. Akherraz, M. Barara are with Mohamed V University, Mohammadia School's of Engineers, Av. Ibn Sina P.B 765 Agdal, Rabat, Morocco (e-mail: abbou@emi.ac.ma, akherraz@emi.ac.ma, mohamed-barara@hotmail.fr).

where the angular frequency ω_s is expressed as follow:

$$\omega_s = \omega_r + \frac{L_m i_{sq}}{T_r \varphi_{rd}} \;;\; \omega_r = p\Omega \tag{2}$$

III. Backstepping Control Design

The backstepping is a recursive and systematic design method for nonlinear and uncertain systems. It allows the construction of control laws from Lyapunov function which ensures the stability of the closed loop dynamic systems. The backstepping procedure is designed from two following steps:

Step1:

Let us define the tracking errors e_1 and e_2 as follow:

$$e_1 = \Omega^* - \Omega \tag{3}$$

$$e_2 = \varphi_{rd}^* - \varphi_{rd} \tag{4}$$

The errors dynamic $\dot{e}_1$ and $\dot{e}_2$ are given by:

$$\dot{e}_1 = \dot{\Omega}^* - \eta\varphi_{rd} i_{sq} + \frac{f}{J}\Omega + \frac{C_r}{J} \tag{5}$$

$$\dot{e}_2 = \dot{\varphi}_{rd}^* + \frac{1}{T_r}\varphi_{rd} - \frac{L_m}{T_r} i_{sd} \tag{6}$$

A Lyapunov function is defined as:

$$V_1 = \frac{1}{2}e_1^2 + \frac{1}{2}e_2^2 \tag{7}$$

The time derivative of V_1 is computed as:

$$\begin{aligned}\dot{V}_1 = &-k_1 e_1^2 - k_2 e_2^2 + e_1\left(k_1 e_1 + \dot{\Omega}^* - \eta\varphi_{rd} i_{sq} + \frac{f}{J}\Omega + \frac{C_r}{J}\right) \\ &+ e_2\left(k_2 e_2 + \dot{\varphi}_{rd}^* + \frac{1}{T_r}\varphi_{rd} - \frac{L_m}{T_r} i_{sd}\right)\end{aligned} \tag{8}$$

where k_1 and k_2 are positive design parameters. To make $\dot{V}_1$ negative definite, the desired value i_{sq}^* and i_{sd}^* are defined as:

$$i_{sq}^* = \frac{1}{\eta\varphi_{rd}}\left(k_1 e_1 + \dot{\Omega}^* + \frac{f}{J}\Omega + \frac{C_r}{J}\right) \tag{9}$$

$$i_{sd}^* = \frac{T_r}{L_m}\left(k_2 e_2 + \dot{\varphi}_{rd}^* + \frac{1}{T_r}\varphi_{rd}\right) \tag{10}$$

Therefore, the derivative of the Lyapunov function (7) becomes such as:

$$\dot{V}_1 = -k_1 e_1^2 - k_2 e_2^2 < 0 \tag{11}$$

The virtual controls in (9) and (10) are chosen to satisfy the objective of regulation and are considered as references for the next step.

Step 2:

Let us define the tracking errors e_3 and e_4 as follow:

$$e_3 = i_{sq}^* - i_{sq} \tag{12}$$

$$e_4 = i_{sd}^* - i_{sd} \tag{13}$$

Substituting the first end second equations of (1) into (12) and (13) respectively, the error dynamics $\dot{e}_3$ and $\dot{e}_3$ are given by:

$$\dot{e}_3 = \dot{i}_{sq}^* - \Psi_1 - \frac{1}{\sigma L_s} v_{sq} \tag{14}$$

$$\dot{e}_4 = \dot{i}_{sd}^* - \Psi_2 - \frac{1}{\sigma L_s} v_{sd} \tag{15}$$

with:

$$\Psi_1 = -\gamma i_{sq} - p\Omega i_{sd} - \mu p\Omega\varphi_{rd} - \frac{L_m}{T_r}\frac{i_{sq} i_{sd}}{\varphi_{rd}} \tag{16}$$

$$\Psi_2 = -\gamma i_{sd} + p\Omega i_{sq} + \frac{\mu}{T_r}\varphi_{rd} + \frac{L_m}{T_r}\frac{i_{sq}^2}{\varphi_{rd}} \tag{17}$$

On the other hand, the (5) and (6) can be expressed as:

$$\dot{e}_1 = -k_1 e_1 - \eta\varphi_{rd} e_3 \tag{18}$$

$$\dot{e}_2 = -k_2 e_2 - \frac{L_m}{T_r} e_4 \tag{19}$$

Let us define the Lyapunov function:

$$V_2 = \frac{1}{2}e_1^2 + \frac{1}{2}e_2^2 + \frac{1}{2}e_3^2 + \frac{1}{2}e_4^2 \tag{20}$$

The time derivative of V_2 is computed as:

$$\begin{aligned}\dot{V}_2 = &-k_1 e_1^2 - k_2 e_2^2 - k_3 e_3^2 - k_4 e_4^2 + e_3\left(k_3 e_3 + \dot{i}_{sq}^* - \Psi_1 - \frac{1}{\sigma L_s} v_{sq} + \eta\varphi_{rd} e_1\right) \\ &+ e_4\left(k_4 e_4 + \dot{i}_{sd}^* - \Psi_2 - \frac{1}{\sigma L_s} v_{sd} + \frac{L_m}{T_r} e_2\right)\end{aligned} \tag{21}$$

where k_3 and k_4 are positive design parameters. To make $\dot{V}_2$ negative definite, the desired value v_{sq}^* and v_{sd}^* are defined as:

$$v_{sq}^{*} = \sigma L_s \left(k_3 e_3 + i_{sq}^{*} - \Psi_1 + \eta \varphi_{rd} e_1 \right) \quad (22)$$

$$v_{sd}^{*} = \sigma L_s \left(k_4 e_4 + i_{sd}^{*} - \Psi_2 + \frac{L_m}{T_r} e_2 \right) \quad (23)$$

The derivative of the Lyapunov (21) becomes:

$$\dot{V}_2 = -k_1 e_1^2 - k_2 e_2^2 - k_3 e_3^2 - k_4 e_4^2 < 0 \quad (24)$$

Then, the error dynamics $\dot{e}_3$ and $\dot{e}_4$ in (14) and (15) can be presented as:

$$\dot{e}_3 = -k_3 e_3 - \eta \varphi_{rd} e_1 \quad (25)$$

$$\dot{e}_4 = -k_4 e_4 - \frac{L_m}{T_r} e_2 \quad (26)$$

Fig. 1 shows the block diagram of the proposed control design.

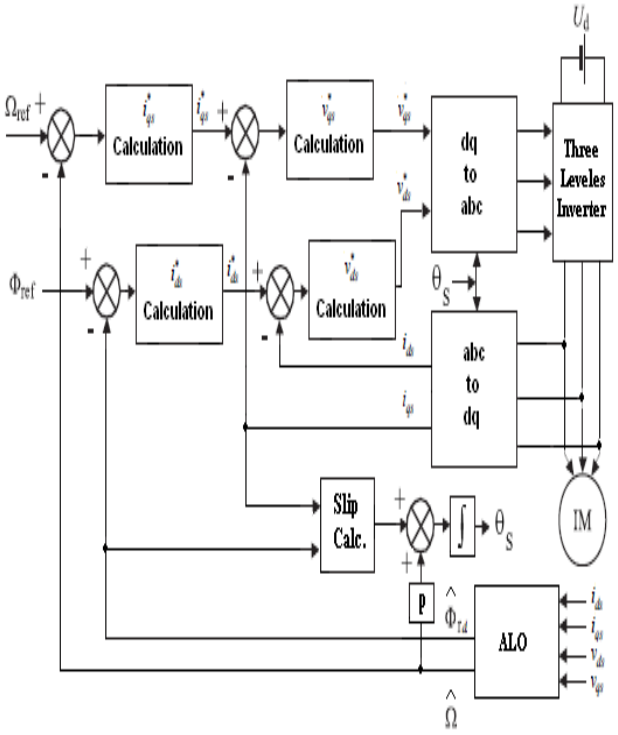

Fig. 1 Diagram of the proposed control design

IV. Three Levels NPC Inverter

Fig. 2 shows the structure of a three levels neural point clamp inverter with three legs [8]. Each leg consists of four switches, the antiparallel diodes and two clamped diodes. The output voltage has three possible values Ud/2, 0 and –Ud/2 corresponding respectively to the states 1, 0 and -1.

Table I shows the switching states available for the three levels inverter of Fig. 2.

TABLE I
Switching States of Three Levels Inverter (X=A, B, C)

States	S_{1X}	S_{2X}	S_{3X}	S_{4X}
1	ON	ON	OFF	OFF
0	OFF	ON	ON	OFF
-1	OFF	OFF	ON	ON

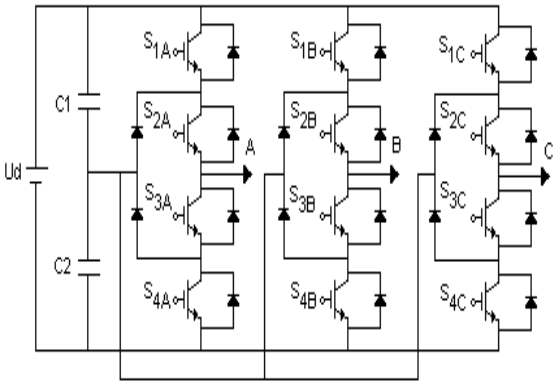

Fig. 2 Basic structure of three levels diode clamped inverter

Fig. 3 shows a hexagon of the voltage vectors for three levels inverters [8]. Each leg can have three switching states, which results in 27 voltage vectors classified as eighteen effective voltage vectors and one zero vector. The zero voltage vector V1 has three switching states, each of the vectors (V2-V7) has two switching states and each of the middle vectors (V9-V11-V13, V15) and the large vectors (V8, V10, V12, V14, V16, V18) has one state.

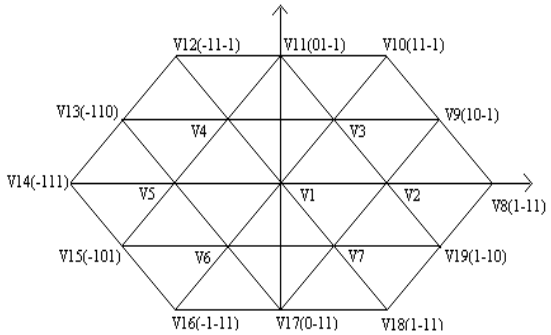

V1(000,111,-1-1-1);V2(100,0-1-1);V3(00-1,110);V4(010,-10-1)
V5(011,-100);V6(001,-1-10);V7(101,0-10)

Fig. 3 Switching states of inverter

V. Adaptive Luenberger Observer

The Adaptive flux observer is a deterministic type of observer based on a deterministic model of the system [7]. In this work, the ALO state observer is used to estimate the flux components and rotor speed of induction motor by including

an adaptive mechanism based on the Lyapunov theory. In general, the equations of the ALO can be expressed as follow:

$$\begin{cases} \dot{\hat{x}} = A\hat{x} + Bu + L(y - \hat{y}) \\ \hat{y} = C\hat{x} \end{cases} \quad (27)$$

The symbol ^ denotes estimated value and L is the observer gain matrix. The mechanism of adaptation speed is deduced by Lyapunov theory. The estimation error of the stator current and rotor flux, which is the difference between the observer and the model of the motor, is given by [9]:

$$\dot{e} = (A - LC)e + \Delta A\hat{x} \quad (28)$$

where:

$$e = x - \hat{x} \quad (29)$$

$$\Delta A = A - \hat{A} = \begin{bmatrix} 0 & 0 & 0 & \mu\Delta\omega_r \\ 0 & 0 & -\mu\Delta\omega_r & 0 \\ 0 & 0 & 0 & -\Delta\omega_r \\ 0 & 0 & \Delta\omega_r & 0 \end{bmatrix} \quad (30)$$

$$\Delta\omega_r = \omega_r - \hat{\omega}_r \quad (31)$$

We consider the following Lyapunov function:

$$V = e^T e + \frac{(\Delta\omega_r)^2}{\lambda} \quad (32)$$

where λ is a positive coefficient. Its derivative is given as follow:

$$\dot{V} = e^T \left\{ (\dot{A} - LC)^T + (A - LC) \right\} e - 2\mu\Delta\omega_r \left(e_{is\alpha}\hat{\varphi}_{r\beta} - e_{is\beta}\hat{\varphi}_{r\alpha} \right) + \frac{2}{\lambda}\Delta\omega_r\dot{\hat{\omega}}_r \quad (33)$$

with $\hat{\omega}_r$ is the estimated rotor speed. The adaptation law for the estimation of the rotor speed can be deduced bye the equality between the second and third terms of (33):

$$\hat{\omega}_r = \int \lambda\mu \left(e_{is\alpha}\hat{\varphi}_{r\beta} - e_{is\beta}\hat{\varphi}_{r\alpha} \right) dt \quad (34)$$

The speed is estimated by a PI controller described as:

$$\hat{\omega}_r = K_p \left(e_{is\alpha}\hat{\varphi}_{r\beta} - e_{is\beta}\hat{\varphi}_{r\alpha} \right) + \frac{K_i}{s} \int \left(e_{is\alpha}\hat{\varphi}_{r\beta} - e_{is\beta}\hat{\varphi}_{r\alpha} \right) dt \quad (35)$$

with K_p and K_i are positive constants. The feedback gain matrix L is chosen to ensure the fast and robust dynamic performance of the closed loop observer [10], [11].

$$L = \begin{bmatrix} l_1 & -l_2 \\ l_2 & l_1 \\ l_3 & -l_4 \\ l_4 & l_3 \end{bmatrix} \quad (36)$$

with l_1, l_2, l_3 and l_4 are given by:

$$l_1 = (d-1)\left(\gamma + \frac{1}{T_r}\right) \;;\; l_2 = -(d-1)\hat{\omega}_r$$

$$l_3 = \frac{(d^2-1)}{\mu}\left(\gamma - \mu\frac{L_m}{T_r}\right) + \frac{(d-1)}{\mu}\left(\gamma + \frac{1}{T_r}\right) \;;\; l_4 = -\frac{(d-1)}{\mu}\hat{\omega}_r$$

where d is a positive coefficient obtained by pole placement approach [12].

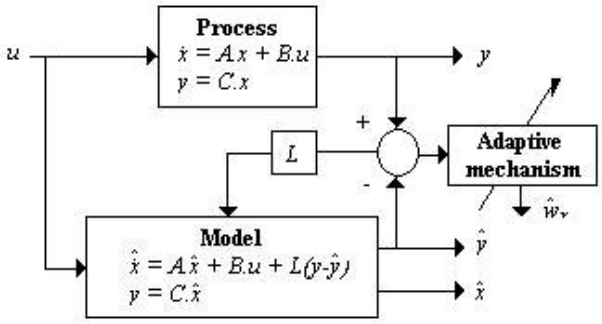

Fig. 4 Block diagram of the adaptive Luenberger observer

VI. Simulation Results

A series of simulation tests were carried out on backstepping approach of induction motor drive based on adaptive flux observer. Simulations have been realized under the Matlab/Simulink. The parameters of induction motor used are indicated in Table II.

TABLE II
INDUCTION MOTOR PARAMETERS

Rated power	3 KW
Voltage	380V Y
Frequency	50 Hz
Pair pole	2
Rated speed	1440 rpm
Stator resistance	2.2 Ω
Rotor resistance	2.68 Ω
Inductance stator	0.229 H
Inductance rotor	0.229 H
Mutual inductance	0.217 H
Moment of Inertia	0.047 kg.m^2
Viscous friction factor	0.004 kg.m^2/s

Fig. 5 shows the simulation responses of the system commanded for 1 Wb of rotor flux and 100 rad/s of rotor speed with the application of a load torque (T_L = 10 Nm) between t = 1s and t = 1.5 s. Fig. 6 shows the simulation responses with steps in speed varying between -100 rad/s and 100 rad/s and we keep constant the rotor flux. In order to

confirm the effectiveness of the proposed control at high and low speed, we made a third and fourth simulations as shown in Figs. 7 and 8.

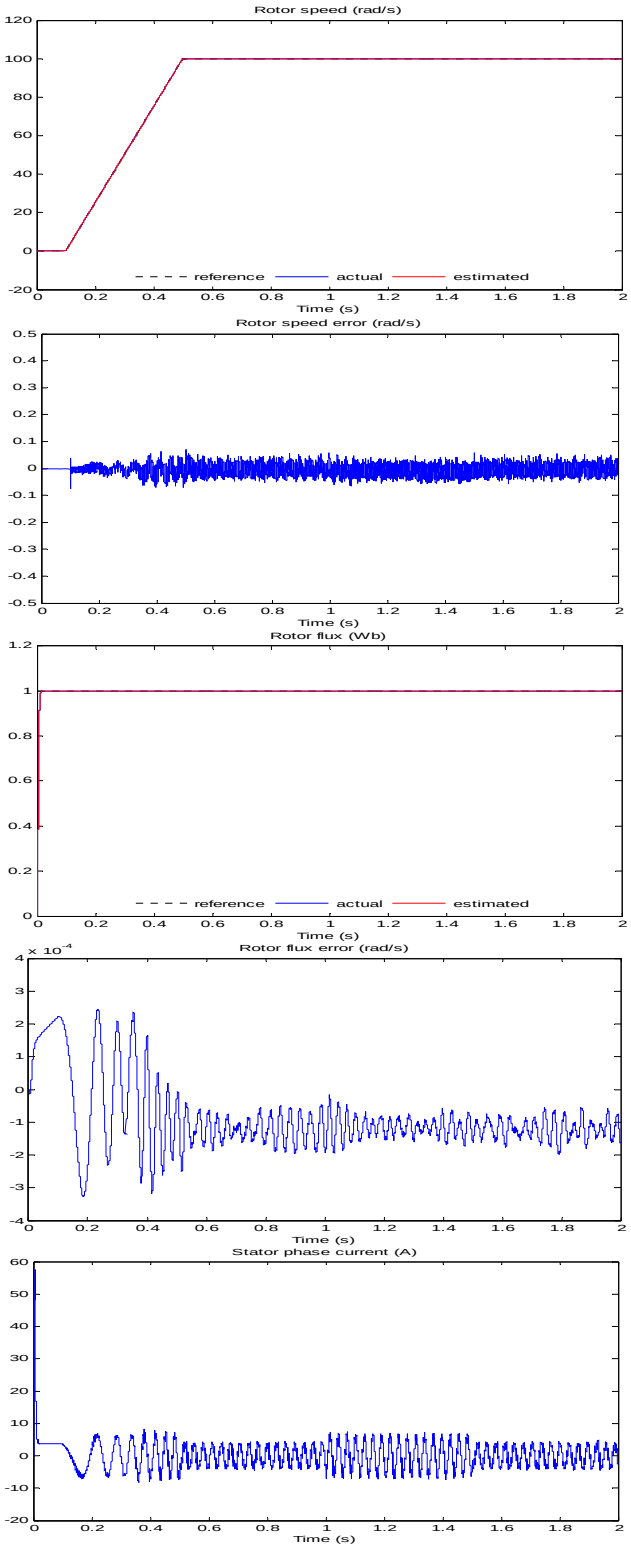

Fig. 5 Simulation responses using ALO observer under load torque

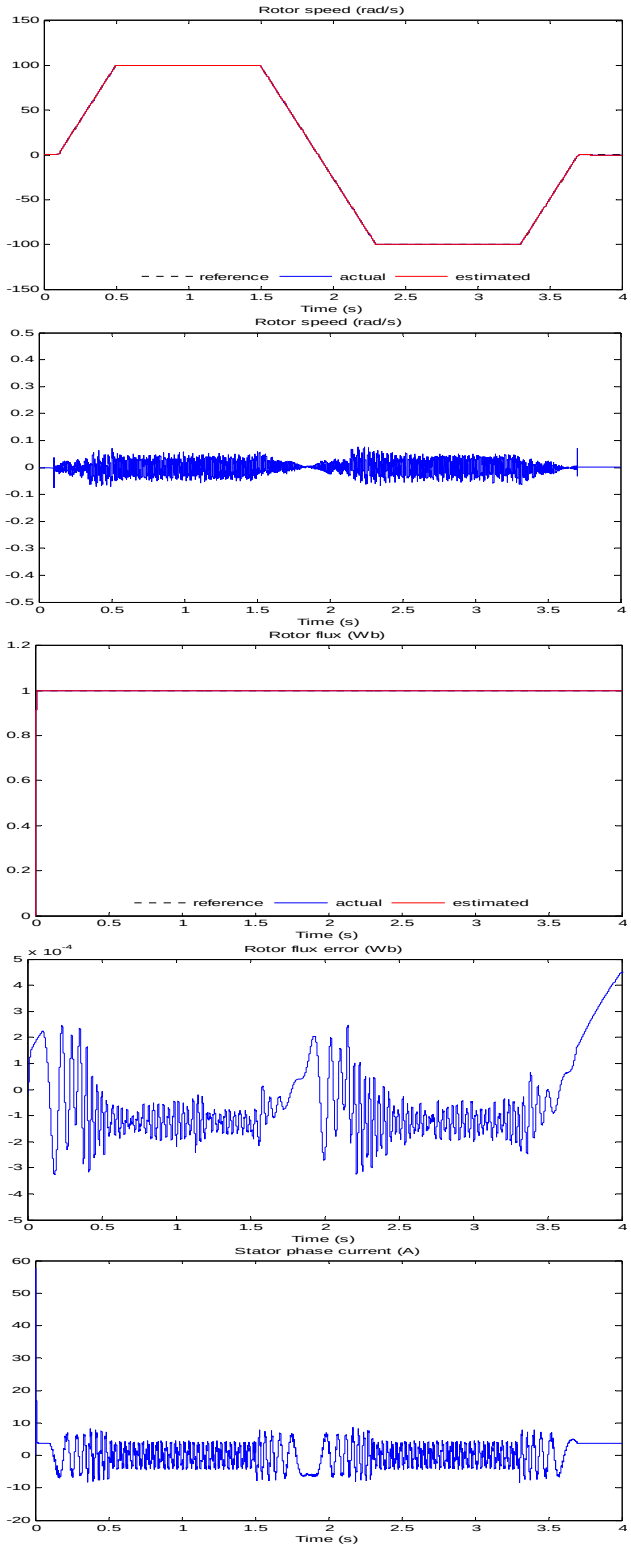

Fig. 6 Simulation responses using ALO observer with a speed reverse

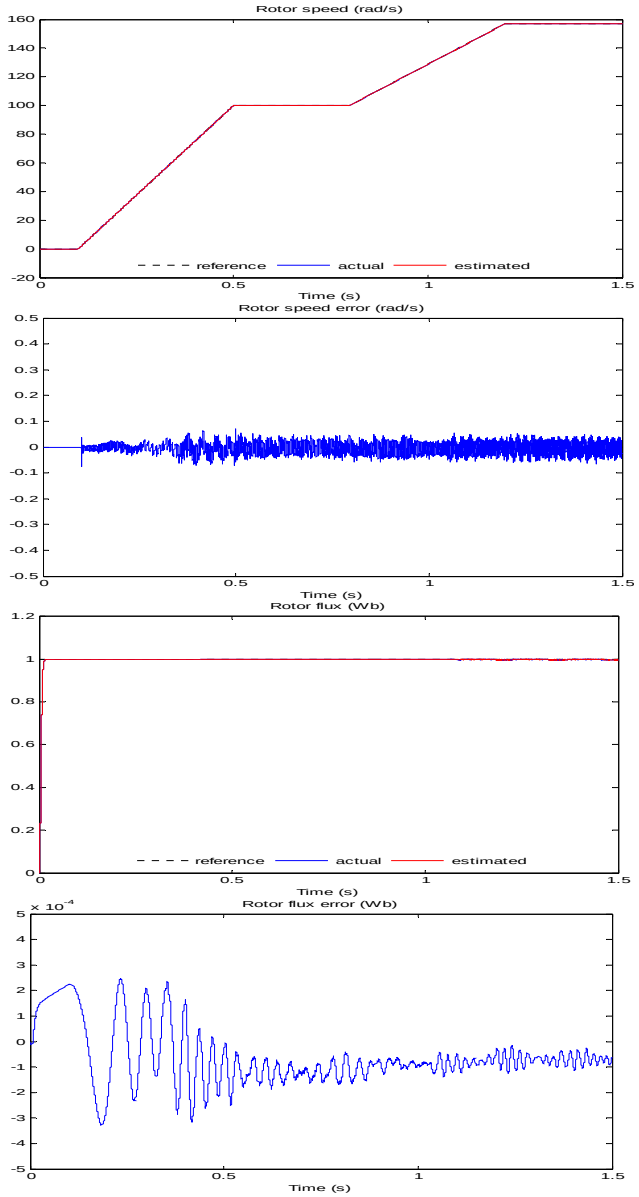

Fig. 7 Simulation responses using ALO observer at high speed

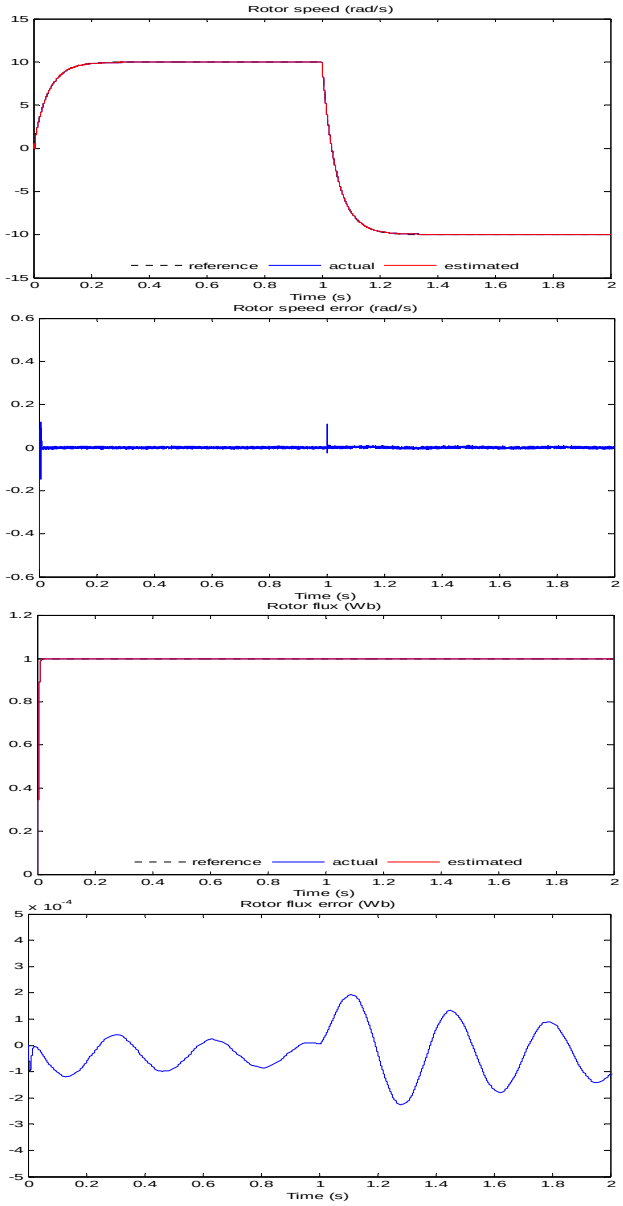

Fig. 8 Simulation responses using ALO observer at low speed

With the results, we can notice the good estimated speed tracking performance test in different working in high and low speed in terms of overshoot, static error and fast response. The flux is very similar to the nominal case. The stator phase current remains sinusoidal and takes appropriate value. It is evident from these simulation results that the proposed backstepping controller presents an excellent performance.

VII. Conclusion

In this paper, we have designed a speed and flux control of the induction motor using a backstepping control approach with adaptive Luenberger observer that provides simultaneous estimation of rotor flux and rotor speed associated with the three levels neutral point clamped inverter. The estimation of the rotor speed is deduced using Lyapunov theory. The simulation results have demonstrated the effectiveness of the proposed scheme for steady state responses of flux and speed even at low and high speed.

References

[1] F. Blaschke, "The principle of field orientation as applied to the new transvector closed loop control system for rotating-field machines,"

Siemens Rev, 34, pp. 217-220, 1972.

[2] R.J Wai , F.J Lin and S.P Hsu, "Intelligent backstepping control for linear induction motor drives," *IEE Proceedings Control Theory and Applications*, Vol. 148, n. 3, pp. 193-202, 2001.

[3] F.J. Lin, R.J. Wai, W.D. Chou and S.P. Hsu, S, "Adaptive backstepping control using tecurrent neural network for linear induction motor Drive," *IEEE Transactions on Industrial Electronics,* Vol. 49, n. 1, pp. 134-146, February. 2002.

[4] N. Ezziani, A. Hussain, N. Essounbouli and A. Hamzaoui, "Backstepping adaptive type-2 fuzzy controller for induction machine," *ISIE,* 2008.

[5] H. Nakano and I. Takahashi, "Sensorless field oriented control of an induction motor using an instantaneous slip frequency estimation method," *IEEE Power Electronics Specialists Conference*, vol. 2, pp. 847-854, 1988.

[6] T. Ohtani, N. Takada and K. Tanaka, "Vector control of induction motor without shaft encoder," *IEEE industry Applications Society Annual Meeting Conference Record,* 1, pp. 500-507, Oct 1989.

[7] Juraj Gacho and Milan Zalman, "IM based speed servodrive with luenberger observer," *Journal of Electrical Engineering,* vol. 6, n. 3, pp. 149–156, 2010.

[8] A. Abbou and H. Mahmoudi, "Performance of a sensorless direct torque flux control strategy for induction motors associated to the three levels npc converter used in electric vehicles", *IJ-STA*, vol. 2, n. 2, pp. 790-803, 2008.

[9] J. Maes and J. Melkebeek, "Speed sensorless direct torque control of induction motor using an adaptive flux observer," *Proc. Of IEEE Trans. Industry Appl,* vol. 36, pp. 778-785, 2000.

[10] S. Belkacem, F. Naceri, A. Betta and L. Laggoune, "Speed sensorless of induction motor based on an improved adaptive flux observer," *IEEE Trans. Industry Appl*, pp. 1192-1197, 2005.

[11] B. Akin, "State estimation techniques for speed sensorless field orient control of induction motors," *M.Sc. Thesis EE Dept, METU,* 2003.

[12] Sio-Iong Ao Len Gelman, "Advances in electrical engineering and computational science lecture," *Notes in Electrical Engineering,* vol. 39, Editors, 2009.

[13] A. Bennassar, A. Abbou, M. Akherraz, M. Barara, "Fuzzy logic speed control for sensorless indirect field control of induction motor using an extended Kalman filter," *IREACO*, vol. 6, n. 3, pp. 332-339, 2013.